RSC Advances

ROYAL SOCIETY OF CHEMISTRY

www.rsc.org/advances

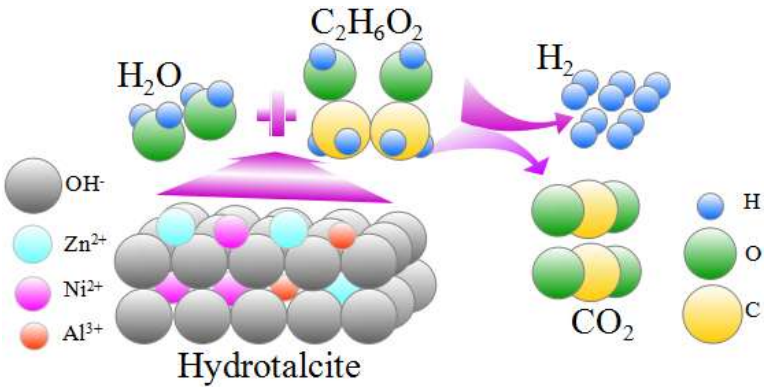

Graphic abstract

The artical illustrates the aqueous-phase reforming of ethylene glycol over Ni/Zn/Al hydrotalcite. The catalytic performance was measured through H_2 selectivity, alkanes selectivity and conversion of ethylene glycol in the products. The effect of reaction conditions on products is also demonstrated. The results of reaction exhibited that the H_2 yield and selectivity were ranged around 73% and 96%, respectively. The conversion of ethylene glycol was over 99%.

Cite this: DOI: 10.1039/c0xx00000x

www.rsc.org/xxxxxx

ARTICLE TYPE

Hydrogen production by aqueous-phase reforming of ethylene glycol over Ni/Zn/Al derived hydrotalcite catalyst

Guanyi Chen[*a,b,c], Ningge Xu[a], Xiangping Li[a], Qingling Liu[a], Huijun Yang[a,d], Wanqing Li[a]

Received (in XXX, XXX) Xth XXXXXXXXX 20XX, Accepted Xth XXXXXXXXX 20XX
DOI: 10.1039/b000000x

Abstract

Ni/Zn/Al hydrotalcites (Ni/Zn/Al-HT) with different Ni/Zn ratio have been prepared by a coprecipitation method. The properties and microstructure of Ni/Zn/Al-HT precursors and derived catalysts were characterized via X-ray diffraction (XRD), H_2-temperature programmed reduction (TPR), N_2 physical adsorption analysis (BET) and scanning electron microscopy (SEM). The result exhibited that the as-prepared samples were consisted of a hydrotalcite phase and a ZnO phase, and Zn^{2+} was introduced in the layers. At the ratio of Ni/Zn=1, the $ZnAl_2O_4$ phase emerged after calcination; Ni still remained as the original status after reaction, but ZnO was always existed during the whole process. In aqueous-phase reforming (APR) of ethylene glycol, the H_2 production rate over Ni/Zn/Al-HT appears a high value, and the selectivity of H_2 can almost reach 100% with a high conversion rate exceeding 99%.

Keywords: Hydrogen, Hydrotalcite, Aqueous-phase reforming, Ethylene glycol, Catalyst

Introduction

Hydrogen is nonpolluting and efficient as a potential desirable energy source. However, nearly 95 % of the world hydrogen energy was produced from fossil fuels at the present[1]. As the depletion of fossil fuel, using renewable sources for hydrogen production is an attractive alternative way. What's more, the production of H_2 from renewable biomass source is environmentally - friendly due to its carbon-neutral nature.

Aqueous-phase reforming (APR) is a lower energy consumption technology for conversion of biomass to hydrogen than steam reforming or gasification which usually occurs at high temperature and was accompanied by many side reactions. It needn't vaporize water and minimizes undesirable decomposition reactions, meanwhile, the water-gas shift reaction (WGS) is active at the low temperature, which is possible to realize generating H_2 and CO_2 in a single step with low levels of CO.

Many oxygenated compounds derived from biomass, such as methanol, ethanol, sorbitol, glycerol and ethylene glycol have been used in APR process[2-8], The mechanism of hydrogen production of ethylene glycol had been researched by Shabaker et al[4, 9, 10]. Ethylene glycol in which each carbon atom bonds to an oxygen atom is capable of being converted to more H_2 and CO_2 by means of C-C scission and WGS reaction. There is not only the process of the cleavage of C-C bonds in the APR, but also involves C-H scission to form adsorbed species on the catalyst surface, such as CO, which is going through water-gas shift to form CO_2. Thus, the catalyst applied to the reaction must be chosen to be favor in the cleavage of C-C and WGS reaction, but should inhibit C-O scission and methanation reactions.

In the past decades, many catalysts (such as supported Pt, Pd, Ru, Rh and Ir) had been tested in APR process. These catalysts with exorbitant price presented good activity and hydrogen selectivity[3-5, 11, 12], but the expensive price prohibited their extensive use. Currently, non-noble based catalysts used for hydrogen production aroused researchers' widespread interest, especially VIII group transition metals. Just as noble metal, the non-noble metal also possesses superior catalytic activity and ability of C-C scission. Skeletal Ni and Sn modified Raney Ni catalysts showed equivalent catalytic effect[11, 13-15], but the steps of synthesizing supported Ni catalysts appeared cumbersome. Thus, it is significantly interesting to develop high efficient catalytic material with low cost and simple prepared method for hydrogen production by APR process of oxygenated hydrocarbons.

Hydrotalcite-like compounds are being the center of interests

[a] *School of Environmental Scinence and Engineering/State Key Laboratory of Engines, Tianjin University, Tianjin 300072, China*
[b] *School of Science, Tibet University, No.36 Jiangsu Street, Lhasa, 850012, Tibet Antonomous Region, China*
[c] *Key Laboratory of Biomass-based Oil and Gas (Tianjin University), China Petrolum and Chimecal Industry Federation, China*
[d] *Key Laboratory of Efficient Utilization of Low and Medium Grade Energy (Tianjin University), Ministy Education, Tianjin 300072, China*

of academics and industrials as layered double hydroxides (LDHs) which include lamellar materials derived from brucite layers[16-19] . These compounds are usually expressed by the formula as: $[M^{2+}_{(1-x)}M^{3+}_{x}(OH)_2]\cdot [A^{n-}]_{x/n}\cdot m\ H_2O$; where M^{2+} is a bivalent cation like Mg^{2+}, Ni^{2+}, Cu^{2+}, Zn^{2+}; M^{3+} is a trivalent cation like Al^{3+}, Fe^{3+}, Mn^{3+}, Cr^{3+}; and A^{n-} is a convertible anion located in the interlayer space for the sake of balancing the positive charge of the layers. The LDHs will become an amorphous metal oxides with small crystal size and high thermal stability by means of heating, which is called ex-LDHs. The ex-LDHs present significant properties such as large surface area, high dispersion of the active metal[16, 20, 21, 22] , the function of memory or the interaction between different cations in the oxides matrix[23, 24] . Furthermore, the small and thermally stable metallic crystalline will be formed through the reduction treatment. Thus, many kinds of hydrotalcite-like compounds have been widely used for hydrogen production in the aqueous-phase reforming of hydrocarbons or alcohols[7, 15, 17, 25] . Pan had demonstrated the catalyst of Ni/Sn/Al derived from hydrotalcite performed well activity in the process of aqueous-phase reforming of ethylene glycol, in which the selectivity of H_2 reached 100%. However, Sn^{2+} wasn't introduced into the layers because of its large ionic radii[25] . The researchers also tested the activity of Ni supported catalysts by reduction of Ni/Mg/Al for aqueous-phase reforming. The Ni/Mg/Al catalyst derived hydrotalcite exhibited a rather high activity as well as high H_2 selectivity (98.84%) , but the catalyst was easily deactivated in the aqueous solutions[26, 27]. Liu reported that Ni/Zn/Al could form well hydrotalcite crystalline with the proper ratio by coprecipitation so that it possessed all the property that hydrotalcite had[28], but their catalysts didn't show any catalytic performance or effects of preparation process on it, because the catalysts didn't be applied to catalyze any reactions.

Herein, the Ni/Zn/Al derived from hydrotalcite was used as catalyst for hydrogen production by the aqueous-phase reforming of ethylene glycol. The performance of H_2 production was tested over Ni/Zn/Al catalysts after reduction. The effects of the atomic ratio Ni/Zn and reaction conditions on the catalytic performance was investigated in detail.

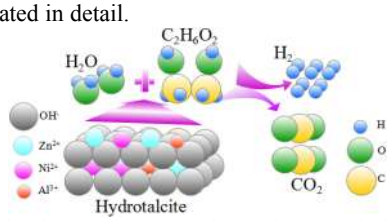

Fig. 1. The sketch map of aqueous-phase reforming of ethylene glycol over hydrotalcite

Experimental

Catalyst preparation

A series of Ni/Zn/Al hydrotalcite-like compounds with different Ni: Zn: Al atomic ratios were synthesized by a coprecipitation method[28]. An aqueous solution (50 mL) containing $Ni(NO_3)_2\cdot 6H_2O$, $Al(NO_3)_3\cdot 9H_2O$ and $Zn(NO_3)_2\cdot 6H_2O$ with the cation concentration of 1 mol/L was added dropwise with vigorous stirring into 50 mL of NaOH and $NaCO_3$ solutions (CO_3^{2-}/Al^{3+}= 0.375 and OH^-/Al^{3+}= 6.3) at ambient temperature. The pH was controlled between 6 and 8, and the resulting slurry was aged at 333 K for 18 h. The precipitate was washed thoroughly with distill water under 100 °C till the pH of the filtrate up to 7, then the samples were dried at 80 °C overnight, crashed and passed through an 80-mesh sieve. The prepared catalysts precursors were designated as Ni/Zn/Al-HT.

Catalyst characterization

The XRD patterns were obtained on a Bruker D8 Advance X-ray diffractometer using Ni-filtered Cu K α radiation(1.5418 Å) with a scanning angle (2θ) of 10-90 °. The voltage was 40 kv, and the current was 40 mA. The Scherrer equation was used to estimate the crystallite size. The textual characteristics, such as BET specific area and pore volume (BJH method), were determined by N_2 physisorption at 77 K. Prior to the analysis the samples were outgassed at 423 K under a N_2 flow for 6 h. The reducibility of the catalysts was analyzed by temperature programmed reduction (TPR), carried out in Autosorb-iQ-C-TCD-MS apparatus. Scanning electron microscope (SEM) measurements were performed with a ZEISS MERLIN Compact microscope. For the sake of removing the surface contaminants, 50 mg of the catalyst was pretreated at 300 °C in a pure N_2 for 3 h, then cooled to the room temperature, and then kept it under 90 % H_2/Ar in the range of 23- 900 °C at a heating rate of 10 °C/min. The amount of H_2 consumed was quantified with a thermal conductivity detector (TCD) equipped with a 5Å molecular sieve to remove H_2 from the effluent gas.

Catalytic activity tests

The catalytic activity test for aqueous-phase reforming (APR) of ethylene glycol was carried out in an autoclave reactor with a capacity of 100 mL, in which there were an 20 wt% aqueous solution and 0.2 g catalyst. Before the test, the catalyst was reduced at 500 °C for 4 h under H_2 flow (50 mL/min), using heating rate of 10 °C/min. The reaction took place at 210-240 °C, and the pressure in the reactor was regulated to 1.95-3.4 MPa with nitrogen gas. The gas products were collected and analyzed by gas chromatograghy (Beifen GC-3420A), equipped with 3 m Porapak Q column and 2 m 5Å molecular sieve (TCD and FID). The products detected were H_2, CO_2, CO, CH_4 and C_2H_6 in the gas phase, which were calculated without considering water for their selectivity. The liquid phases were analyzed by Agilent 7890A 60 m DB-Wax capillary column. The analysis result presented that liquid products mainly contained un-reacted ethylene glycol, methanol and acetic acid. The data were collected for up to 3 h for each set of reaction condition taking into account the performance of APR in order to assure that the catalyst system reached steady state.

H_2 selectivity was calculated by hydrogen amounts of H_2/ total carbon amounts of gas products$\times \frac{1}{R}$, where R was the H_2/CO_2 reforming ratio of 5/2 for ethylene glycol; alkane selectivity was calculated by carbon amounts of alkane/ total carbon amounts of gas products.

Results and discussion

Structure analysis of hydrotalcite precursors

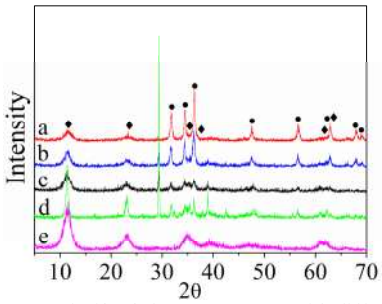

Fig.2. XRD patterns of Ni/Zn/Al-HL precursors with different Ni/Zn ratio. (a) $Ni_{0.8}Zn_{3.2}Al$; (b) $Ni_{1.33}Zn_{2.66}Al$; (c)Ni_2Zn_2Al; (d)$Ni_{2.66}Zn_{1.33}Al$; (e) $Ni_{3.2}Zn_{0.8}Al$. (◆): hydrotalcite; (●): ZnO

It's of vital importance to detect that whether the as prepared Ni/Zn/Al-HT samples form the hydrotalcite phase, so the XRD patterns of it are shown in Fig. 2 (Fig. 2: (Ni+ Zn)/ Al=4, and Ni/ Zn= 0.25, 0.5, 1, 2, 4 respectively) . Only the precursor of Ni/Zn=4 formed a single hydrotalcite phase, while in the case that Ni/Zn ⩽ 2, a ZnO phase was observed obviously and accompanied with a hydrotalcite phase. Liu reported that the precursors could form a hydrotalcite phase when the ratio of Ni/Zn was between 0.25 and 4, at the same time the ratio of (Ni+ Zn)/Al equaled to 4~6[28], Fig. 2 shows the similar result. The formation of ZnO can be ascribed to that more spare Zn^{2+} formed $Zn(OH)_2$ when the ratio of Ni/Zn is smaller than the ratio in the desired hydrotalcite $Zn(OH)_2$ is converted to ZnO through drying out because of its easy dehydration[29]. The interlayer space (*dc*) of Ni/Zn/Al-HT (Ni/Zn=0.25, 0.5, 1, 2, 4) is 7.7402, 7.6448, 7.7330, 7.7221, 7.7017 Å, respectively. Thus it can be seen that the value of *dc* decreases with the content of Zn^{2+} decreasing, which illustrates that the Zn^{2+} is introduced in the layer. Several parameters of hydrotalcite can be calculated by the follow functions[30] :

Cell parameter $a= \sqrt{2}\,[(1-x)d_{M(II)-O} + xd_{M(III)-O}]$ (1)

Electronic density of layer $q_c= 2xe/(\sqrt{3}\cdot a^2)$ (2)

In which, x=M(Ⅲ)/(M(Ⅱ)+M(Ⅲ)); $d_{M(II)-O}$, $d_{M(III)-O}$ represent the distances between M(Ⅱ) or M(Ⅲ) and oxygen, respectively. Because the smaller radius of Ni^{2+} than Zn^{2+} (Zn^{2+}=0.88 Å, Ni^{2+}=0.83 Å) attributed to the value of a decreasing, the electronic density of layer increased[20] . Space of the interlayer relates to the electronic density of interlayer anion coordination. The increasing value of q_c means that the interaction between Ni^{2+} and anion becomes stronger than Zn^{2+} and anion with the content of Ni^{2+} increasing. Thus, the interlayer space decreases successively[31] . As a result, it can be explained that Zn^{2+} has been introduced in the layer.

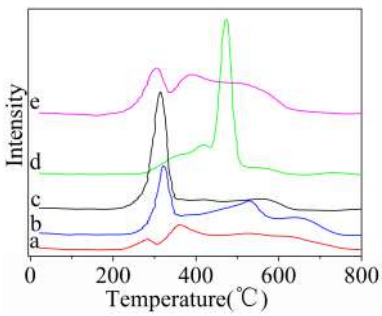

Fig.3. H_2-TPR profiles of Ni/Zn/Al hydrotalcite. (a) $Ni_{0.8}Zn_{3.2}Al$; (b) $Ni_{1.33}Zn_{2.66}Al$; (c)Ni_2Zn_2Al; (d)$Ni_{2.66}Zn_{1.33}Al$; (e) $Ni_{3.2}Zn_{0.8}Al$.

The results of H_2-TPR analysis of catalysts with different Ni/Zn ratio are shown in Fig. 3. It is apparent that every catalyst has an obvious main reductive peak between 217 and 513 °C. As is shown in Fig. 3, the low temperature reductive peaks are between 217 and 356 °C for all the catalysts except $Ni_{2.66}Zn_{1.33}Al$. However, the H_2 consumption reductive peak of $Ni_{2.66}Zn_{1.33}Al$ appears at 473 °C with two shoulder peaks around 349 and 419 °C, respectively. Wang reported that single NiO would reduce at 375 °C with H_2 consumed[32] ; For our catalysts, the reductive temperature of NiO shows lower than that. This case is supposed that the NiO reduced already in our catalysts is divided into two kinds: one that can be reduced easily under low temperature is weak interaction with other oxides or free; and the other that needs higher reductive temperature interacts with other oxides strongly under enough content of Ni in catalysts. Moreover, $ZnAl_2O_4$ will be showed up in calcined catalysts when the content of Ni is adequate[33] . Thus, the low temperature reductive peaks between 217 and 435 °C in every catalyst ascribe to the reduction of the first kind of NiO demonstrated before, although there was a shoulder peak between 267 °C and 381 °C in $Ni_{2.66}Zn_{1.33}Al$; the high temperature reductive peaks between 309 and 585 °C in the four catalysts except Ni_2Zn_2Al are due to the reduction of the other kind of NiO, it's likely that all the NiO had been reduced at the same time period in Ni_2Zn_2Al so as to forming the reductive peak of NiO with the strongest intensity; the third shoulder peaks between 448 and 778 °C in the three catalysts, the second shoulder peaks between 467 and 648 °C in Ni_2Zn_2Al and the main reductive peak between 435 and 531 °C in $Ni_{2.66}Zn_{1.33}Al$ is attributed to the reduction of Al^{3+} probably. More content of Ni causes the intensity of H_2 consumption peak at 304 °C of $Ni_{3.2}Zn_{0.8}Al$ becoming weak, because the quantity of NiO that could be reduced decreased. The Ni^{2+} was introduced into $ZnAl_2O_4$ formed as demonstrated before in stead of Zn^{2+}, thereupon it got hardly reduced as the same as Zn^{2+}.

Table1 Chemical composition, textural characteristics of the reductive catalysts with different Ni/Zn derived from hydrotalcite

Samples	BET (m^2/g)	Pore volumn (cm^3/g)	Pore size (nm)
$Ni_{0.8}Zn_{3.2}Al$	37.40	0.16	53.08
$Ni_{1.33}Zn_{2.66}Al$	26.08	0.09	15.90
Ni_2Zn_2Al	7.42	0.03	21.72
$Ni_{2.66}Zn_{1.33}Al$	3.58	0.01	17.14
$Ni_{3.2}Zn_{0.8}Al$	18.91	0.08	21.72

Table 1 listed the BET (BJH method) results of Ni/Zn/Al-HT catalysts with different Ni/Zn ratio. $Ni_{0.8}Zn_{3.2}Al$ has the biggest surface area, pore volume and pore size. The surface area decreases gradually with the increase of Ni content.

Table 2 Catalytic performance of Ni/Zn/Al-HL derived catalysts with different Ni/Zn.

Samples	Gas phase composition				H_2 sel%	Alkanes sel %	Conversion %
	H_2 %	CO_2 %	CH_4 %	C_2H_6 %			
$Ni_{0.8}Zn_{3.2}Al$	72.74	20.28	0	1.74	95.58	21.35	99.85
$Ni_{1.33}Zn_{2.66}Al$	73.20	22.28	1.95	0.77	100	12.70	99.74
Ni_2Zn_2Al	79.95	18.10	0.77	0.36	100	7.36	99.27
$Ni_{2.66}Zn_{1.33}Al$	70.24	28.13	0.33	0.21	93.77	2.50	99.82
$Ni_{3.2}Zn_{0.8}Al$	67.05	24.54	6.71	0.67	79.75	23.93	99.87

[a]Reactant variety: 20 wt% solution of ethylene glycol; reaction temperature and pressure: 225 °C, 2.6 MPa.

Catalytic performance

The aqueous-phase reforming reaction of ethylene glycol is mainly through the pathway of C-C cleavage and WGS reaction to produce H_2 as shown in Fig 4. Meanwhile, some side reactions also happen, which generate side products like C_2H_6, C_2H_5OH and so on.

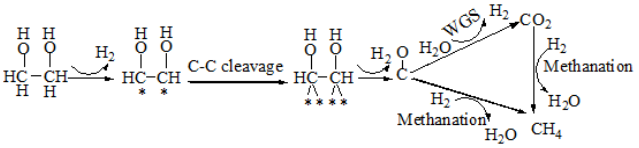

Fig. 4. Part reaction pathways from reaction of ethylene glycol with water (*represents a surface metal site)[3]

In our reaction, the H_2 production and selectivity increase from 72.74 % first, and then decline to 67.05 % with the contents of Ni increasing, as is shown in Table 2. However, the yield of CO_2 and alkanes selectivity present opposite tendency. The phenomenon can be attributed to the high content of metal, which may contribute to catalyst deactivation because of the aggregation of metallic particles partly. It can be seen that the alkanes selectivity reaches the most (23.93 %) when the Ni content increases to Ni/Zn=4, which illustrates that methanation reaction will be strengthened with enough Ni. Optimistically, all conversion of ethylene glycol is over 99 %. It is obvious that the catalyst with Ni/Zn=1 possesses the best catalytic ability. The H_2 selectivity reaches 100 %, the alkanes selectivity is as low as 7.36 % and the content of H_2 in the gas product is 79.95 %. The case is probably supposed that moderate content of Ni will promote the cleavage of C-C to the greatest extent, and weaken the methanation reaction as well. In addition, some crystal may form, which is also to the benefit of H_2 production. So it is chosen for further investigation.

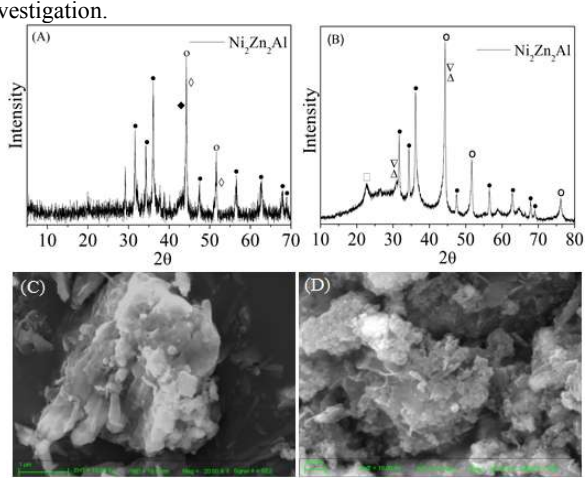

Fig.5. XRD and SEM patterns of Ni_2Zn_2Al derived hydrotalcite. (A) after reduction; (B) after reaction; (C) after reduction; (D)after reaction. (●):ZnO; (◆):NiO; (○):Ni; (◇):$AlNi_3$; (△):AlNi; (▽):$Al_{0.96}Ni_{1.04}$; (□):H_2O

XRD and SEM analysis of catalysts

Three oxides had been formed in the Ni_2Zn_2Al derived hydrotalcite after calcination: the wurtzite type phase (ZnO), the rock salt type phase (NiO) and the spinel phase ($ZnAl_2O_4$), which corresponds to the report given by Resini. C[20]. At the same time, the crystalline of Al_2O_3 was highly dispersed in the whole calcining process[28]. The component of NiO in the calcined catalyst probably was reduced to Ni thereby playing a great part in promoting hydrogen production[25] . The result of XRD patterns after reduction is shown in Fig. 5(A). It can be clearly seen that metal Ni was formed as expected at 39.45, 46.84, 71.3 ° with the crystalline of AlNi and $AlNi_3$ alloy formed at the same time. As demonstrated before, ZnO is hardly to reduce Zn^{2+}, so the phase of ZnO can still be detected. The H_2 production and catalytic activity are probably facilitated by ZnO as well.

However, some crystalline may change with the reaction happening. Fig. 5(B) shows the XRD result of Ni_2Zn_2Al derived hydrotalcite after reaction. The composition of catalyst contains mainly Ni, ZnO, H_2O and AlNi alloy with different ratios. The catalyst still remains the component activated to H_2, which is considered as a factor to have ability to recycle. The SEM pattern of Ni_2Zn_2Al derived hydrotalcite after reduction is exhibited in Fig. 5(C). The structure is composed of three phase: porous Ni-rich compact regions occupied much of the pattern, nanorod of ZnO regions around the Ni-rich regions and crystalline regions sticking to the Ni-rich regions containing AlNi alloy with different ratios[34, 35] . As suggested in Fig. 5, the Ni-rich regions still remained after exposure to aqueous-phase reforming reaction conditions, which displays in Fig. 5(D). However, the nanorod of ZnO is adhered to much crystalline of AlNi and $Al_{0.96}Ni_{1.04}$ alloy, which is difficult to be observed. The SEM results are corresponded to the XRD patterns apparently.

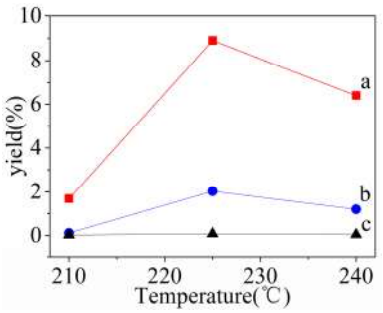

Fig.6. Effect of temperature on the catalytic performance of APR using Ni_2Zn_2Al hydrotalcite derived catalyst. (a) H_2;(b) CO_2; (c) CH_4. Reactant variety: 20 wt% ethylene glycol aqueous solutions, reaction temperature and pressure: 210 °C, 1.95 MPa; 225 °C, 2.6 MPa; 240 °C, 3.4 MPa.

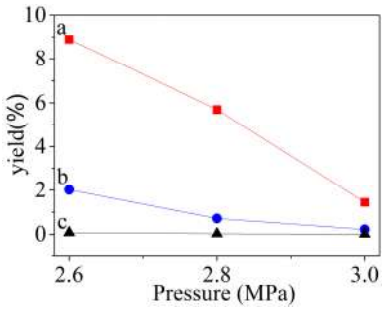

Fig.7. Effect of pressure on the catalytic performance of APR using Ni_2Zn_2Al hydrotalcite derived catalyst. (a) H_2; (b) CO_2; (c) CH_4. Reactant variety: 20 wt% ethylene glycol aqueous solutions, reaction temperature: 225 °C; pressure: 2.6 MPa; 2.8 MPa; 3.0 MPa.

Effects of reaction conditions over Ni_2Zn_2Al-HT

The influences of reaction temperature and pressure on the yield rate of H_2, CO_2 and CH_4 over Ni_2Zn_2Al hydrotalcite derived catalyst is shown in Fig. 6-7.

Fig. 6 indicates that the best result appears at 225 °C. The content of H_2 in the gas product grows up from 1.68 to 8.9 % with the temperature increasing from 210 to 225 °C, then declines to 6.4 % when the reaction temperature increases to 240 °C. The H_2 selectivity reaches nearly 100 %, and the methane selectivity increases from 7.36 to 32.95 %, following on dropping to 5.38 %. With increasing of reaction temperature, it appears that CO and CO_2 in the gas product both take the methanation reaction with H_2; meanwhile, the water-gas shift reaction is weakened.

As illustrated in Fig. 7, H_2 production decreases from 8.9 to 1.45 % when the pressure increases from 2.6 to 3.0 MPa. The H_2 selectivity remains nearly 79 %, and alkanes selectivity reaches 12 %. With reaction pressure rising, the partial pressure of H_2 in the gas product increases, thus, the equilibrium of chemical reaction moves reversely and the rate of reaction decreases in consequence; moreover, the increasing of pressure results in the rate of H_2 and CO desorption from the catalyst catalytic site decreasing, so it is more likely to take methanation reaction, which leads to in H_2 production decreasing[36, 37].

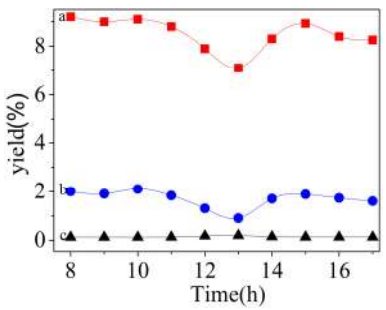

Fig.8. Catalytic stability of Ni_2Zn_2Al hydrotalcite derived catalysts. (a)H_2; (b)CO_2; (c)CH_4. Reactant variety: 20 wt% ethylene glycol aqueous solutions; reaction temperature and pressure: 225 °C, 2.6 MPa.

The catalytic performance versus time on the stream for aqueous-phase reforming of 20 wt% ethylene glycol over Ni_2Zn_2Al hydrotalcite derived catalyst is exhibited in Fig 8. It is apparent that the catalytic activity exists the tendency of declining, but the deactivation phenomenon doesn't sustain too long, otherwise the degree of deactivation isn't dramatic either. Resini C reported that the catalytic activity of $Ni_{50}ZnAl$-HT decreased after 500min in the process of ethanol steam reforming[20] . Therefore, further studies are needed to investigate the mechanism of deactivation and the effect of Ni/Zn ratio.

Conclusion

Ni/Zn/Al hydrotalcite (Ni/Zn/Al-HT) catalysts with different ratios of Ni/Zn are synthesized by a coprecipitation method. The results present that Zn^{2+} was introduced in the layers. XRD patterns suggest that the as-prepared samples was composed by a hydrotalcite phase and a ZnO phase. ZnO may be in favor of H_2 selectivity and catalytic activity in aqueous-phase reforming of ethylene glycol. A high H_2 production yield, a good H_2 selectivity of 100 % and a high conversion in excess of 99 % are showed over Ni_2Zn_2Al. Ni/Zn/Al-HT appears very interesting in potential application for aqueous-phase reforming reaction due to its easy fabrication and good performance.

Acknowledgments

This paper is financially sopprted by National Basic Research Program of China through 973 Program (2012CB215303).

References

1 D. S, *Int J Hydrogen Energy*, 2002, **27**, 235-264.
2 R. D. Cortright, R. R. Davda and J. A. Dumesic, *Nature*, 2002, **418**, 964-967.
3 R. R. Davda, J. W. Shabaker, G. W. Huber, R. D. Cortright and J. A. Dumesic, *Appl Catal B*, 2005, **56**, 171-186.
4 J. W. Shabaker, R. R. Davda, G. W. Huber, R. D. Cortright and J. A. Dumesic, *J Catal,* 2003, **215**, 344-352.
5 J. W. Shabaker, G. W. Huber, R. D. Cortright and J. A. Dumesic, *Catal Lett,* 2003, **88**, 1-7.
6 R. R. Soares, D. A. Simonetti and J. A. Dumesic, *Angew Chem Int Ed,* 2006, **45**, 3982-3985.
7 I. O. Cruz, N. F. P. Ribeiro, D. A. G. Aranda and M. M. V. M. Souza, *Catal Commun,* 2008, **9**, 2606-2611.
8 P. V. Tuza, R. L. Manfro, N. F. P. Ribeiro and M. M. V. M. Souza, *Renew Ener*, 2013, **50**, 408-414.
9 J. W. Shabaker, J. A. Dumesic and Ind., *Angew Chem Int Ed*, 2004, **43**, 3105-3112.
10 A. B, J. a. P. D and Vaidya, *Energy Fuels*, 2015, **29**, 361-368.
11 G. W. Huber, J. W. Shabaker and J. A. Dumesic, *Science,* 2003, **300**, 2075-2077.
12 B. a. Kaya, S. Irmak, A. H. glu and O. Erbatur, *Hydrogen Energy*, 2015, **40**, 3849-3858.
13 F. Xie, X. Chu, H. Hu, M. Qiao, S. Yan, Y. Zhu, H. He, K. Fan, H. Li, B. Zong and X. Zhang, *J Catal,* 2006, **241**, 211-220.
14 J. W. Shabaker, G. W. Huber and J. A. Dumesic, *J Catal,* 2004, **222**, 180-191.
15 J. W. Shabaker, D. A. Simonetti, R. D. Cortright and J. A. Dumesic, *J. Catal*, 2005, **231**, 67-76.
16 F. Cavani, F. Trifiro and A. Vaccari, *Catal Today*, 1991, **11**, 173-301.
17 W. Feitknecht, *Helv Chim Acta* 1942, **25**, 555-569.
18 M. Li, X. Wang, S. Li, S. Wang and X. Ma, *Int J Hydrogen Energy*, 2010, **35**, 6699-6708.
19 S. Miyata, *Clay Clay Miner*, 1983, **31**, 305-311.
20 C. Resini, T. Montanari, L. Barattini, G. Ramis, G. Busca, S. Presto and e. al., *Appl Catal A Gen*, 2009, **355**, 83-93.
21 L. Dussault, J. C. Dupin, E. Dumitriu, A. Auroux and C. Guimon, *Thermochim Acta,* 2005, **434**, 93-99.
22 S. H. Sarijo, S. A. I. S. M. Ghazali and M. Z. Hussein, *J Porous Mater*, 2015, **22**, 473-480.
23 V. Mas, M. L. Dieuzeide, M. Jobba´gy, G. Baronetti, N. Amadeo and M. Laborde, *Catal Today*, 2008, **133**, 319-323.
24 O. Meyer, F. Roessner, R. A. Rakoczy and R. W. Fischer, *ChemCatChem*, 2010, **2**, 314.
25 G. Pan, Z. Ni, F. Cao and X. Li, *Appl Clay Sci*, 2012, **58**, 108-113.
26 G. Pan, Z. Ni, F. Cao and X. L. 1328-32, *J Chin Ceram Soc*, 2010, **38**, 1328-1332.
27 G. Pan, F. Cao, Z. Ni, X. Li, H. Chen, B. Tang and M. Xu, *Chin Ceram Soc*, 2011, **39**, 33-37.
28 J. Liu and X. Xie, *J Fuel Chem Techno,* 2001, **29**, 69-72.
29 T. Chen, M. Zhou, L. Wang and Z. Zhan, *Chin J Syn Chem,* 2002, **10**, 45-48.
30 Z. Ni, G. Pan, L. Wang, C. Fang and D. Li, *Chin J Inor Chem,* 2006, **22**, 91-95.
31 L. Ren, F. Li, J. He and X. Duan, *J B Univ Chem Technol*, 2002, **29**, 77-79.
32 Y. Wang, Dalian university of technology, 2007.
33 Z. Zhou, A. Zhang, M. Gong and Y. Chen, *Chem Res Appl*, 2000, **12**, 521-524.
34 J. Dong, F. Zhang, W. Zhang and YanningYang, *J Funct Mater Devic*, 2011, **36**, 657-660.
35 J. Chen and Z. Xu, *ShangHai Nonferr Met,* 2003, **24**, 12-15.
36 Y. Bai, C. Lu, L. Ma, P. Chen, Y. Zheng and X. Li, *Chinese J Catal,* 2006, **27**, 275-280.

37 J. Xie, X. Yin, D. Su, C. Wu and J. Zhu, *Trans Chin Soc Agri Mech*, 2011, **42**, 104-110.